Generalized fractional diffusion equations for accelerating subdiffusion and truncated Lévy flights

A. V. Chechkin,[1] V. Yu. Gonchar,[1] R. Gorenflo,[2] N. Korabel,[3] and I. M. Sokolov[4]
[1]*Institute for Theoretical Physics NSC KIPT, Akademicheskaya street, 1, 61108 Kharkov, Ukraine*
[2]*Institute of Mathematics, Free University of Berlin, Arnimallee 3, D-14195 Berlin-Dahlem, Germany*
[3]*Physics Department, Bar-Ilan University, Ramat-Gan 52900, Israel*
[4]*Institute of Physics, Humboldt University, Newtonstrasse 15, D-12489 Berlin, Germany*
(Received 25 January 2008; published 12 August 2008)

Fractional diffusion equations are widely used to describe anomalous diffusion processes where the characteristic displacement scales as a power of time. For processes lacking such scaling the corresponding description may be given by diffusion equations with fractional derivatives of distributed order. Such equations were introduced in A. V. Chechkin, R. Gorenflo, and I. Sokolov [Phys. Rev. E **66**, 046129 (2002)] for the description of the processes getting more anomalous in the course of time (decelerating subdiffusion and accelerating superdiffusion). Here we discuss the properties of diffusion equations with fractional derivatives of the distributed order for the description of anomalous relaxation and diffusion phenomena getting less anomalous in the course of time, which we call, respectively, accelerating subdiffusion and decelerating superdiffusion. For the former process, by taking a relatively simple particular example with two fixed anomalous diffusion exponents we show that the proposed equation effectively describes the subdiffusion phenomenon with diffusion exponent varying in time. For the latter process we demonstrate by a particular example how the power-law truncated Lévy stable distribution evolves in time to the distribution with power-law asymptotics and Gaussian shape in the central part. The special case of two different orders is characteristic for the general situation in which the extreme orders dominate the asymptotics.

DOI: 10.1103/PhysRevE.78.021111 PACS number(s): 05.40.−a, 05.10.Gg, 05.40.Fb

I. INTRODUCTION

"Normal" kinetic processes are described by the Fick's diffusion equation, a parabolic partial differential equation for the probability density function (PDF) $p(x,\ t)$ of finding a particle at site x at time t:

$$\frac{\partial}{\partial t}p(x,t) = D\frac{\partial^2}{\partial x^2}p(x,t), \quad D > 0. \tag{1}$$

This equation was first obtained by Fick in 1855 on the basis of what we would now call linear response theory, and the underlying microscopic picture was understood by Einstein fifty years later. The diffusive behavior follows as a continuous limit of random walks, in which the overall particle's displacement up to time t can be represented as a sum of independent random steps, in the case that both the mean squared displacement per step and the mean time needed to perform a step are finite. The Fick's equation is invariant under the scale transformation $x \to \lambda x$, $t \to \lambda^2 t$, so that the characteristic scale of its solution (diffusion length) grows as $L \propto t^{1/2}$. In many cases, however, the characteristic displacement scales as

$$L \propto t^{\mu} \tag{2}$$

with $\mu \neq 1/2$ or does not scale at all. In these cases one often speaks about anomalous kinetics. The prominent examples of the scaling anomalous behavior are the Lévy flights and the continuous-time random walks with power-law waiting-time distributions (see [1,2]). These are described by fractional-order kinetics, i.e., through diffusion equations with the fractional, instead of the first- or second-order derivative in its temporal or spatial variable, respectively. In the first case, the *time-fractional diffusion equation* with the *Caputo fractional derivative* on the left-hand side,

$$\frac{\partial^{2\mu}}{\partial t^{2\mu}}p(x,t) = D\frac{\partial^2}{\partial x^2}p(x,t) \tag{3}$$

$(0 < \mu < 1/2)$ for subdiffusion or, in the second case, the *space-fractional diffusion equation*, with the *Riemann-Liouville* or *Riesz* derivative on the right-hand side,

$$\frac{\partial}{\partial t}p(x,t) = D\frac{\partial^{1/\mu}}{\partial x^{1/\mu}}p(x,t) \tag{4}$$

$(\mu > 1/2)$ for superdiffusion guarantee the proper scaling, Eq. (2). However, the form with the temporal *Riemann-Liouville* derivative,

$$\frac{\partial}{\partial t}p(x,t) = D\frac{\partial^{1-2\mu}}{\partial t^{1-2\mu}}\frac{\partial^2}{\partial x^2}p(x,t) \tag{5}$$

$(0 < \mu < 1/2)$ for subdiffusion or

$$\frac{\partial^{2-1/\mu}}{\partial x^{2-1/\mu}}\frac{\partial}{\partial t}p(x,t) = D\frac{\partial^2}{\partial x^2}p(x,t) \tag{6}$$

$(\mu > 1/2)$ with the spatial *Riemann-Liouville* or *Riesz* derivative for superdiffusion, do this as well. In Eqs. (3)–(6) the fractional derivatives are meant in a generic way, to be specified later; here we only state that the ones in Eqs. (5) and (6) are conjugated to those in Eqs. (3) and (4), and they are all invariant under the scale transformation $x \to \lambda x$, $t \to \lambda^{1/\mu} t$. In Eqs. (3) and (4) the fractional derivatives stand at their "correct" places, i.e., at places where the corresponding ordinary derivative should stay in the Fick's equation. Therefore we

call such forms the "*natural*" form of fractional diffusion equations. The forms (5) and (6) are called *modified* fractional diffusion equations. As long as the scaling situation is considered, the forms (3) and (5) as well as Eqs. (4) and (6), respectively, are equivalent and give rise to the same solutions (under proper definition of the corresponding derivatives) [3].

However, many systems demonstrate anomalous *nonscaling* behavior, which corresponds either to crossover between different power laws, or to a non-power-law behavior as exemplified by the logarithmic growth of the distribution width. As examples of such nonscaling situations we can refer to truncated Lévy flights in the superdiffusive case [4,5] and to Sinai-like superslow diffusion [6] in the subdiffusive case. For these two examples it was shown that the behavior of the corresponding PDFs can be described by diffusion equations with *distributed-order derivatives* [7,8]. For ordinary differential equations distributed-order derivatives were originally introduced by Caputo [9–11] for generalizing stress-strain relation of inelastic media. An example of such diffusion equation was first discussed in [12], where the connection of such equation for subdiffusion with the corresponding continuous-time random walk (CTRW) scheme was also established. The distributed-order derivative is nothing else but a linear operator defined as a weighted sum of different fractional derivatives or an integral of such over their order, $\int_a^b d\beta p(\beta)\frac{\partial^\beta}{\partial z^\beta}$, acting on the function of the corresponding variable z. In the case of distributed-order diffusion equations z means time or space. Such equations are the versatile instrument for the description of nonscaling anomalous diffusion processes, as shown by the corresponding examples in Refs. [7,8,13,14]. Once again, depending on the position of the fractional operator, the corresponding distributed-order equation can be of natural or of modified form. The natural forms were discussed in detail in our previous papers. We also note that such distributed-order fractional diffusion equations find more and more interest among "pure" mathematicians, who proved rigorously the results stated in our previous works, and developed the corresponding formalism [15–17]. Therefore in the present paper we concentrate on the modified forms.

In the present paper we discuss the properties of such modified equations and present generic examples elucidating the behavior of the corresponding processes. We study the evolution of the solutions of modified distributed order equations with both temporal and spatial fractional derivatives in more detail, showing, e.g., the peculiarities of transformation of the "anomalous" solution at small times into the "normal" solution at long times.

We moreover discuss experimental findings in different fields, such as biophysics, plasma physics, and econophysics, where the effects of transformation from anomalous diffusion behavior to a normal one are observed. Such effects can be phenomenologically described within the framework of distributed-order diffusion equations of modified form.

The paper consists of two large sections. In Sec. II we consider the diffusion equation with time fractional derivative of distributed order in the right-hand side of the equation. In Sec. III we consider the diffusion equation with space fractional derivative of the distributed order in the left side of the equation. In each section a generic particular case is considered with the weight function being a sum of two delta functions with two different exponents, the one of them corresponding to normal diffusion. In both sections solutions of the Cauchy problem are obtained in the Fourier-Laplace domain, and mean squared displacements and probability densities to stay at the origin are evaluated.

II. MODIFIED DISTRIBUTED-ORDER TIME FRACTIONAL DIFFUSION EQUATION

A. General equations

The time-fractional diffusion equation with a distributed-order Riemann-Liouville derivative in the right-hand side was introduced in [3] and reads as

$$\frac{\partial f}{\partial t} = \int_0^1 d\beta p(\beta) K(\beta) {}_0D_t^{1-\beta} \frac{\partial^2 f}{\partial x^2}, \tag{7}$$

where $[K(\beta)]=\mathrm{cm}^2/\mathrm{sec}^\beta$, $p(\beta)$ is a dimensionless nonnegative weight function, and ${}_0D_t^\mu$ is the Riemann-Liouville fractional derivative on the right semiaxis, which for a "sufficiently well-behaved" function $\phi(t)$ is defined as follows:

$${}_0D_t^\mu \phi = \frac{d}{dt} J^{1-\mu}\phi = \frac{1}{\Gamma(1-\mu)}\frac{d}{dt}\int_0^t d\tau \frac{\phi(\tau)}{(t-\tau)^\mu}, \quad 0 \le \mu < 1, \tag{8}$$

where $J^\alpha \phi(t) = 1/\Gamma(\alpha)\int_0^t d\tau (t-\tau)^{\alpha-1} f(\tau)$, $t>0, \alpha \in \mathbf{R}^+$ is the fractional Riemann-Liouville integral. Equation (7) is subject to the initial condition $f(x,t=0)=\delta(x)$. If we set $p(\beta)=\delta(\beta-\beta_0), 0<\beta_0<1$, then we arrive at the time fractional diffusion equation in the modified form,

$$\frac{\partial f}{\partial t} = K_{\beta_0} {}_0D_t^{1-\beta_0} \frac{\partial^2 f}{\partial x^2}. \tag{9}$$

The way we put down Eq. (7) depending on the product $p(\beta)K(\beta)$ leaves some freedom in defining $p(\beta)$ and $K(\beta)$. To comply with dimension of $K(\beta)$ we define it as $K(\beta)=D\tau^{1-\beta}$, where D has a dimension of normal diffusion coefficient, $\mathrm{cm}^2/\mathrm{sec}$, and τ has the dimension of time. As soon as the numerical value of D is fixed, the value of τ is chosen in such a way that the function $p(\beta)$ is normalized, $\int_0^1 d\beta p(\beta)=1$, and can be interpreted as a probability density. The combination $\sqrt{D\tau}$, having the dimension of length, will appear repeatedly in what follows.

We note that Eq. (7), just like Eq. (9), admits a thermodynamical interpretation as a combination of a continuity equation $\partial f/\partial t = -\partial j/\partial x$ and a retarded linear response equation $j(x,t)=\Phi(t)\{\partial f(x,t)/\partial x\}$ for the flux exhibiting memory of the process at previous times $t'<t$ [18]. We point out the analogy of this flux dependent on the past history to the flux for a space-fractional diffusion process which is non-local in space [19]. We also note that the natural form of a distributed-order time-fractional diffusion equation does not immediately allow for such a thermodynamical interpretation.

The usual way to deal with fractional diffusion equations is to use Fourier-Laplace transformation techniques. Applying to Eq. (7) the Laplace and Fourier transform in succession, $\tilde{g}(s)=\int_0^\infty dt\ e^{-st}g(t)$, $\hat{g}(k)=\int_{-\infty}^\infty dk\ e^{ikx}g(x)$,

$$\hat{\tilde{f}}(k,s)=\int_{-\infty}^{\infty}dx\ e^{ikx}\int_0^\infty dt\ e^{-st}f(x,t), \tag{10}$$

and taking into account that the Laplace transform of the Riemann-Liouville derivative ${}_0D_t^\mu\phi(t)$ is $s^\mu\tilde{\phi}(s)$, if $J^{1-\mu}\phi(t\to 0)=0$, in particular whenever $\phi(0)$ is finite [20–22], we get

$$\hat{\tilde{f}}(k,s)=\frac{I_{\mathrm{RL}}}{s(I_{\mathrm{RL}}+k^2D\tau)}, \tag{11}$$

where

$$I_{\mathrm{RL}}(s\tau)=\left[\int_0^1 d\beta(s\tau)^{-\beta}p(\beta)\right]^{-1}. \tag{12}$$

Note that Eq. (11) is exactly the same as the equation for the Fourier-Laplace transform of the solution for the natural form, if we replace $I_{\mathrm{RL}}(s\tau)$ by $I(s\tau)=\int_0^1 d\beta(s\tau)^\beta p(\beta)$, see Eq. (6) in [12]. This gives us a solution in terms of the integral formula of subordination, Eq. (10) of Ref. [12]. In both cases, the one described by the modified as well as by the natural distributed-order form, the parent process is the Wiener process; the properties of the operational time (directing process), however, are different in these two cases.

After inverse Fourier transformation of Eq. (11) we obtain

$$\tilde{f}(x,s)=\frac{1}{2\sqrt{D\tau}}\frac{\sqrt{I_{\mathrm{RL}}}}{s}\exp\left(-\sqrt{\frac{I_{\mathrm{RL}}}{D\tau}}|x|\right). \tag{13}$$

The fundamental solution of the Cauchy problem for the modified distributed order equation, Eq. (7), was recently obtained in [23,22] both in terms of the integral of a Laplace type and in terms of a Mellin-Barnes integral. Also, a power series for the solution comes out whose coefficients are time-dependent functionals of the probability density $p(\beta)$. In what follows the two quantities will be of particular interest, namely, (i) probability density to stay at the origin, which reads as

$$f(0,t)=\mathbf{L}_s^{-1}\{\tilde{f}(0,s)\}=\frac{1}{2\sqrt{D\tau}}\mathbf{L}_s^{-1}\left\{\frac{\sqrt{I_{\mathrm{RL}}}}{s}\right\}, \tag{14}$$

where $\mathbf{L}_s^{-1}$ denotes an inverse Laplace transformation with respect to the variable s, and (ii) *mean squared displacement* (MSD), which is given by

$$\langle x^2(t)\rangle=\mathbf{L}_s^{-1}\left\{\left(-\frac{\partial^2\hat{\tilde{f}}}{\partial k^2}\right)_{k=0}\right\}=2D\tau\mathbf{L}_s^{-1}\left\{\frac{1}{sI_{\mathrm{RL}}}\right\}. \tag{15}$$

B. Generic case of double-order equation

In what follows we consider the special form of the probability density $p(\beta)$,

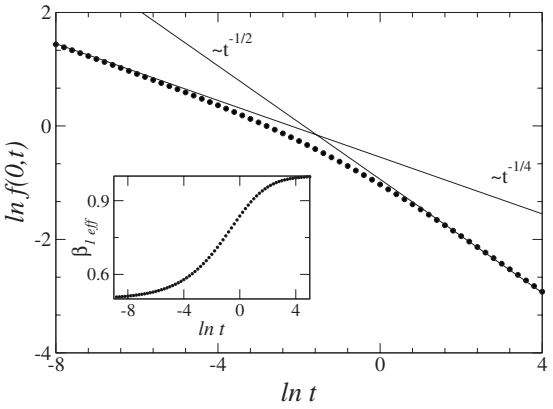

FIG. 1. Main figure: the probability density to stay at the origin obtained from Eq. (18) by numerical inverse Laplace transformation is shown by dots. Parameters: $\beta_1=0.5$, $\beta_2=1$, $b_1=b_2=0.5$. Note the use of dimensionless time and space coordinates. The solid lines show asymptotics $\propto t^{-1/4}$ and $\propto t^{-1/2}$, for small and large times, respectively. Inset: $\beta_{1\mathrm{eff}}$ vs time obtained from the probability density to stay at the origin.

$$p(\beta)=B_1\delta(\beta-\beta_1)+B_2\delta(\beta-\beta_2) \tag{16}$$

with $0<\beta_1<\beta_2\leq 1$, $B_1>0$, $B_2>0$, $B_1+B_2=1$. The corresponding diffusion equation is called *double-order time-fractional diffusion equation* in what follows. This choice allows us to show in a simple way the property of the diffusive behavior governed by distributed order diffusion equations. Inserting Eq. (16) into Eq. (12) gives

$$I_{\mathrm{RL}}(s\tau)=(b_1s^{-\beta_1}+b_2s^{-\beta_2})^{-1}, \tag{17}$$

where $b_1=B_1/\tau^{\beta_1}$, $b_2=B_2/\tau^{\beta_2}$. The positivity of the solution of the double-order time-fractional diffusion equation was proved in [3]. The solution itself was obtained analytically in Ref. [23] in terms of infinite series of the Fox functions. The corresponding random process can be considered as an approximation for a continuous-time random walk (CTRW) process with the waiting-time distribution function $\Psi(t)=1-(b_1\tau^{\beta_1}+b_2\tau^{\beta_2})^{-1}$, and simulated accordingly. The derivation of the corresponding modified diffusion equation from the CTRW theory is considered in Ref. [13].

Probability density to stay at the origin. Inserting Eq. (17) into Eq. (14) we get

$$f(0,t)=\frac{1}{2\sqrt{D\tau}}L_s^{-1}\left\{\frac{1}{s\sqrt{b_1s^{-\beta_1}+b_2s^{-\beta_2}}}\right\}, \tag{18}$$

and, using Tauberian theorems [24],

$$f(0,t)\approx\begin{cases}\dfrac{1}{2\sqrt{D\tau b_1}}\dfrac{t^{-\beta_1/2}}{\Gamma\left(1-\dfrac{\beta_1}{2}\right)}, & t\to 0\\[2ex] \dfrac{1}{2\sqrt{D\tau b_2}}\dfrac{t^{-\beta_2/2}}{\Gamma\left(1-\dfrac{\beta_2}{2}\right)}, & t\to\infty\end{cases}. \tag{19}$$

In Fig. 1 we demonstrate the evolution of $f(0,t)$ obtained by numerical inverse Laplace transformation [25] for $\beta_1=0.5$,

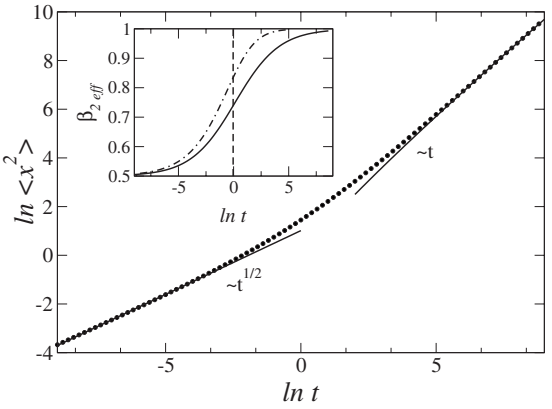

FIG. 2. Main figure: MSD $\langle x^2\rangle$ vs t is shown by dots in the log-log scale. Parameters: $\beta_1=0.5$, $\beta_2=1$, $b_1=b_2=0.5$, $D=\tau=1$. The solid lines show asymptotics $\propto t^{-1/4}$ and $\propto t^{-1/2}$, for small and large times, respectively. The transition from subdiffusion to normal diffusion behavior is clearly seen. Inset: the effective diffusion exponent $\beta_{2\text{eff}}$ obtained from the local slope of the MSD curve is shown by the solid line. For $t=1\beta_{2\text{eff}}(t)=0.74$. Dashed-dotted line demonstrates $\beta_{1\text{eff}}$ from the inset of Fig. 1.

$\beta_2=1$. Note that in all our figures we use dimensionless time (measured in units of τ) and dimensionless length (measured in units of $\sqrt{D\tau}$), which fixes the values of D and τ equal to 1. The dotted curve in the main figure shows the transition from behavior at small times where the smallest exponent dominates, to the behavior at large times, where the largest exponent dominates. The slopes of the dotted curve at very small and very large times are determined by the smallest and largest β values, respectively. The inset shows $\beta_{1\text{eff}}$ defined by the *local* slope. As we proceed to show, $\beta_{1\text{eff}}(t)$ determines the behavior of the PDF at time t with good accuracy, e.g., we may look at the evolution of the probability density to stay at the origin as governed by the exponent $\beta_{1\text{eff}}$, which *varies in time*: $f(0,t)\sim t^{\beta_{1\text{eff}}(t)}$.

Mean squared displacement. Inserting Eq. (17) into Eq. (15) gives by inverse Laplace transformation exactly

$$\langle x^2(t)\rangle = \frac{2D_1}{\Gamma(1+\gamma)}\left(\frac{t}{\tau}\right)^{\beta_1} + \frac{2D_2}{\Gamma(1+\alpha)}\left(\frac{t}{\tau}\right)^{\beta_2}, \qquad (20)$$

where $D_1=B_1D\tau, D_2=B_2D\tau$. Since $0<\beta_1<\beta_2\leq 1$, at small times the first term on the right-hand side of Eq. (20) prevails, whereas at large times the second one dominates. Thus our Eq. (20) describes *accelerating subdiffusion*. We note that this behavior is opposite to the case of decelerated subdiffusion considered in Ref. [12] [see Eqs. (18) and (20) there], where at small times the larger exponent prevails whereas at large times the smaller one dominates.

In Fig. 2 we plot the mean squared displacement (MSD) $\langle x^2\rangle$ as function of t, Eq. (20), with $\beta_1=0.5$, $\beta_2=1$. The dotted line in the main figure shows evolution of the MSD from subdiffusive behavior at small times, where the smallest exponent dominates, to the normal behavior at large times, where the largest exponent dominates. The slopes of the dotted curve at very small and very large times are determined by the smallest and largest values of β, respectively. The inset demonstrates the following property similar to that observed in Fig. 1: at each time instant we may evaluate some $\beta_{2\text{eff}}$ defined by the *local* slope of the MSD curve and shown here by solid line, which governs evolution *exactly* at this instant. In other words, we may look at the evolution of the MSD as governed by the exponent $\beta_{2\text{eff}}$, which *varies in time*: $\langle x^2(t)\rangle\propto t^{\beta_{2\text{eff}}(t)}$. For the comparison, in the inset $\beta_{1\text{eff}}$ vs t is depicted by the dashed-dotted line. One can see that the behavior of both effective exponents is very similar and leads us to the following observation: *the system governed by the distributed-order time-fractional diffusion equation with two diffusion exponents has the properties very similar to the system whose exponent varies in time*. Up to now, we illustrated this statement by demonstrating the evolution of the first return to the origin and the MSD. Now, we turn to the PDF.

Probability density function: Analytical results. For the Laplace transform of the PDF we get from Eqs. (13) and (17)

$$\tilde{f}(x,s) = \frac{1}{2\sqrt{Db_2\tau}}\frac{1}{s^{1-\beta_2/2}\sqrt{1+\frac{b_1}{b_2}s^{\beta_2-\beta_1}}} \times\exp\left[-\frac{|x|}{\sqrt{D\tau b_2}}\frac{s^{\beta_2/2}}{\sqrt{1+\frac{b_1}{b_2}s^{\beta_2-\beta_1}}}\right]. \qquad (21)$$

We begin with two degenerated cases that actually describe single order processes.

Particular case 1: $B_1=\beta_1=0$, $B_2=\beta_2=1$. From Eq. (21) we get

$$\tilde{f}(x,s) = \frac{1}{2\sqrt{Ds}}\exp\left[-\sqrt{\frac{s}{D}}|x|\right], \qquad (22)$$

and, taking into account the Laplace transform pair,

$$\frac{e^{-a\sqrt{s}}}{\sqrt{s}} = \int_0^\infty dt\, e^{-st}\frac{e^{-a^2/4t}}{\sqrt{\pi t}},$$

we arrive at the Gaussian law,

$$f(x,t) = \frac{\exp(-x^2/4Dt)}{\sqrt{4\pi Dt}}. \qquad (23)$$

Particular case 2: $B_1=\beta_1=0$, $B_2=1$, $\beta_2\equiv\beta\leq 1$. From Eq. (21) we get

$$\tilde{f}(x,s) = \sqrt{\frac{\tau}{4D}}\frac{1}{(s\tau)^{1-\beta/2}}\exp\left[-\frac{|x|}{\sqrt{D\tau}}(s\tau)^{\beta/2}\right], \qquad (24)$$

which after inverse Laplace transformation gives

$$f(x,t) = \frac{1}{2\pi i}\int_{Br} ds\, e^{st}\tilde{f}(x,s)$$
$$= \sqrt{\frac{\tau}{4D}}\frac{1}{2\pi i}\int_{Br}\frac{ds}{(s\tau)^{1-\beta/2}}e^{st-(|x|(s\tau)^{\beta/2}/\sqrt{D\tau})}$$
$$= \frac{1}{2\sqrt{D\tau^{1-\beta}}t^{\beta/2}}M\left(\zeta;\frac{\beta}{2}\right), \quad (25)$$

where

$$M(\zeta;\mu) = \frac{1}{2\pi i}\int_{Ha}\frac{d\sigma}{\sigma^{1-\mu}}e^{\sigma-\zeta\sigma^{\mu}}, \quad \zeta = \frac{|x|}{\sqrt{D\tau^{1-\beta}}t^{\beta/2}} \quad (26)$$

is the integral definition of the Mainardi ($M-$) function, *Ha* is the Hankel path [26,27]. We remind that the Hankel path is a loop starting from $-\infty$ along the lower side of the negative real axis, encircles the circular area $|\sigma|=\varepsilon\to 0$ in the positive sense, and ends at $-\infty$ along the upper side of the negative real axis. The Mainardi function can be also defined by the following series representation valid on the whole axis:

$$M(\zeta;\mu) = \sum_{n=0}^{\infty}\frac{(-\zeta)^n}{n!\,\Gamma[-\mu n+(1-\mu)]}$$
$$= \frac{1}{\pi}\sum_{n=1}^{\infty}\frac{(-\zeta)^{n-1}}{(n-1)!}\Gamma(\mu n)\sin(\mu n\pi). \quad (27)$$

Note that the case $\mu=1/2$ corresponds to

$$M(\zeta;1/2) = \pi^{-1/2}\exp(-\zeta^2/4). \quad (28)$$

Thus setting $\beta=1$ in Eq. (25) and using Eq. (28) we arrive at the Gaussian law, Eq. (23).

Let us turn back to the general equation (21) with $0<\beta_1<\beta_2\le 1$. We are interested in the case $\beta_2=1$. Denoting $\beta_1=\beta$, $b_1=b_\beta=B_\beta/\tau^\beta$, $b_2=B/\tau=b$, we rewrite Eq. (21) in equivalent form,

$$\tilde{f}(x,s) = \frac{1}{2\sqrt{Db\tau}}\frac{1}{s^{1/2}\sqrt{1+(b_\beta/b)s^{1-\beta}}}$$
$$\times\exp\left[-\frac{|x|}{\sqrt{D\tau b}}\frac{s^{1/2}}{\sqrt{1+(b_\beta/b)s^{1-\beta}}}\right] \quad (29)$$

[note that for $b_\beta=0$, $b=1$ we again arrive at Eq. (22)]. In accordance with the two particular cases presented above we consider large and small s expansions of Eq. (29) and compare with the particular cases 1 and 2.

Behavior for large s (small t). From Eq. (29) we get

$$\tilde{f}(x,s) \approx \frac{1}{2\sqrt{Db_\beta\tau}}\frac{1}{s^{1-\beta/2}}\exp\left[-\frac{|x|s^{\beta/2}}{\sqrt{Db_\beta\tau}}\right]$$
$$= \sqrt{\frac{\tau}{4DB_\beta}}\frac{1}{(s\tau)^{1-\beta/2}}\exp\left[-\frac{|x|}{\sqrt{DB_\beta\tau}}(s\tau)^{\beta/2}\right] \quad (30)$$

[compare with Eq. (24)]. Thus, after inverse Laplace transformation, we arrive at Eqs. (25) and (26) with substitution of D by DB_β:

$$f(x,t) \approx \frac{1}{2\sqrt{K_\beta}t^{\beta/2}}M\left(\zeta;\frac{\beta}{2}\right), \quad t\to 0, \quad (31)$$

where

$$\zeta = \frac{|x|}{\sqrt{K_\beta}t^{\beta/2}}, \quad K_\beta = DB_\beta\tau^{1-\beta}. \quad (32)$$

The M function exhibits stretched exponential behavior at large values of an argument [26],

$$M(r/\nu,\nu) \approx a(\nu)r^{(\nu-1/2)/(1-\nu)}\exp[-b(\nu)r^{1/(1-\nu)}], \quad (33)$$

where

$$a(\nu) = \frac{1}{\sqrt{2\pi(1-\nu)}}, \quad b(\nu) = \frac{1-\nu}{\nu}$$

[note the reduced argument in Eq. (33)]. In our terms $\zeta=r/\nu$, $\nu=\beta/2$, and Eq. (33) is written as

$$M\left(\zeta,\frac{\beta}{2}\right) \approx \frac{1}{2\sqrt{\pi(2-\beta)}}\left(\frac{2}{\beta}\right)^{1-\beta/2-\beta}\zeta^{-(1-\beta/2-\beta)}$$
$$\times\exp\left\{-\frac{2-\beta}{2}\left(\frac{\beta}{2}\right)^{\beta/2-\beta}\zeta^{2/2-\beta}\right\}. \quad (34)$$

Note that the asymptotics of the solution (31) and (34) was obtained for the first time from the CTRW picture in the problem of subdiffusion in intermittent maps [28].

Behavior for small s (large t). Small s expansion of Eq. (29) gives

$$\tilde{f}(x,s) \approx \frac{1}{2\sqrt{Db\tau s}}\exp\left[-\sqrt{\frac{s}{Db\tau}}|x|\right]$$
$$= \frac{1}{2\sqrt{DBs}}\exp\left[-\sqrt{\frac{s}{DB}}|x|\right] \quad (35)$$

[compare with Eq. (22)]. Thus, after inverse Laplace transformation, we arrive at Eq. (23), with substitution of D by DB:

$$f(x,t) \approx \frac{\exp(-x^2/4DBt)}{\sqrt{4\pi DBt}}, \quad t\to\infty. \quad (36)$$

Probability density function: Numerical results. In numerical simulation the PDF is obtained by the inverse Laplace transformation performed numerically from Eq. (29) with the use of the algorithm presented in [25]. The M function is calculated via its series representation, Eq. (27). In simulations $\beta=0.5$, $D=\tau=1$, $B_\beta=B=0.5$. The results are shown in Figs. 3–5.

In Fig. 3 the solution of a double-order time-fractional diffusion equation is shown at small times for three time instants, 0.002, 0.01, and 0.1. The single-order approximation at small times, Eq. (31), is shown by solid lines for the same instants. The approximation works well at small times. With time increasing, the deviations between exact and approximate solutions grow and become more pronounced on the tail of the PDF, which is clearly shown in the main figure in a logarithmic scale.

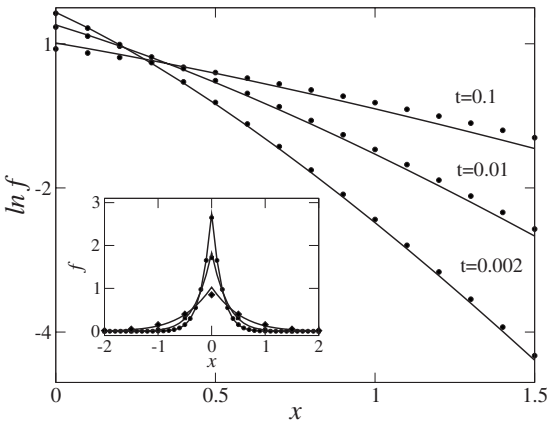

FIG. 3. PDFs at small times. Main figure: the inverse Laplace transform of Eq. (29) is shown in a logarithmic scale for $t=0.002$, 0.01, and 0.1, respectively. The corresponding single-order approximation in terms of the M function, Eq. (31), is shown by solid lines. It is seen that at small times the M function gives a good approximation to the exact solution, and with t increasing the logarithmic discrepancy becomes larger. In the inset the central parts of the PDFs are shown in a linear scale.

The evolution at large times shown in Fig. 4 is in some sense the reverse: with the time increasing the deviations between the exact solution and its single-order Gaussian approximation, Eq. (36), decrease. Again, logarithmic scale used in the main figure allows us to follow how the approximate solution approaches the exact one.

Approximation by single-order solution in the whole time domain. Let us return to the observation made in numerical simulations with probability density to stay at the origin and with MSD, that the double-order diffusion equation has the properties similar to that of single-order equation with exponent varying with time. We pose the question: is it possible to approximate the solution of double-order diffusion equation by the solution of a single-order with time-dependent exponent? In order to make such approximation it is reasonable at first to have at least an empirical rule for how this time-dependent exponent might be chosen, especially keeping in mind the existence of another adjustable parameter D. Below we present two ways to make the approximation.

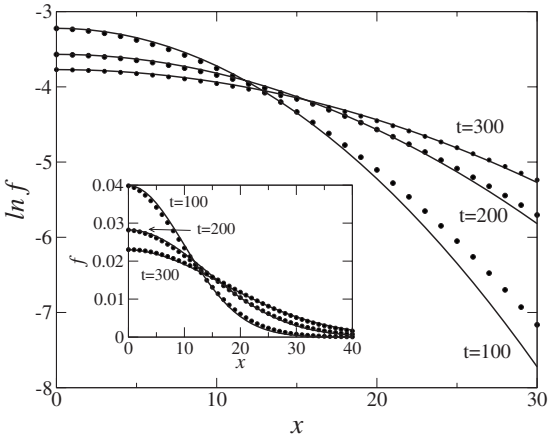

FIG. 4. PDFs at large times. Main figure: the inverse Laplace transform of Eq. (29) is shown in a logarithmic scale for $t=100$, 200, and 300, respectively. The corresponding Gaussians, Eq. (36), are shown by solid lines. It is seen that with t increasing the logarithmic discrepancy between Gaussian approximation and exact solution becomes smaller. In the inset the central parts of the corresponding PDFs are shown in a linear scale.

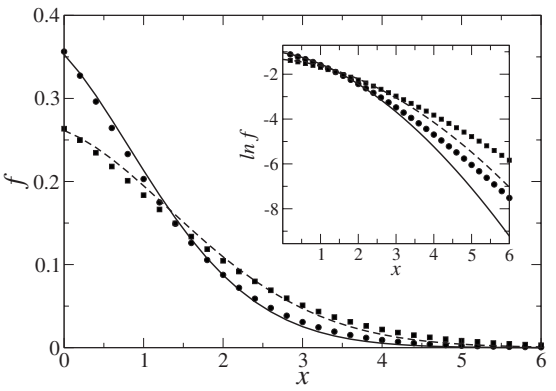

FIG. 5. PDF obtained by inverse Laplace transformation of Eq. (29) is shown by dots for $t=1$ and by squares for $t=2$, in linear and logarithmic scale in the main figure and the inset, respectively. Parameters are the same as in Figs. 3 and 4. Solid line: single-order solution, Eq. (25), taken at $t=1$, with the *effective values* of the parameters β and D. The former equals $\beta_{1\text{eff}}=0.84$; the value is taken from the curve in the inset of Fig. 1 at $t=1$, whereas the latter $D_{\text{eff}}=1.7$ is chosen so as to provide the best fit to exact solution depicted by dots. Dashed line: single-order solution, Eq. (25), taken at $t=2$, with the effective value $\beta_{\text{eff}}=0.9$, taken from the inset of Fig. 1 at $t=2$; again, $D_{\text{eff}}=1.5$ is chosen to provide the best fit to exact solution depicted by squares.

The first one uses $\beta_{1\text{eff}}$ defined from the probability of first return, see Fig. 1. That is, for each time instant t we calculate the value of single-order solution, Eq. (25), with instant value $\beta(t)=\beta_{1\text{eff}}(t)$, the latter is determined from the inset in Fig. 1. Then, we vary parameter D to provide the best fit to the exact solution of double-order equation. The result for intermediate times is shown in Fig. 5. It can be seen, especially from the inset, that for intermediate times the exact solution can be approximated by the single-order solution with the effective values of β and D. Naturally, during the time evolution, β varies between 0.5 and 1, and increases as t grows. The discrepancy between the exact solution and its approximation becomes more visible in the wings of the PDF shown in a logarithmic scale. In general, we may conclude that our choice of the effective β provides a reasonable agreement between single-order approximation and exact solution.

Even better agreement can be achieved if we do not use an effective value of β, but instead try to vary both parameters, β and D, in order to provide the best fit. This point is illustrated in Fig. 6. To put the functions for $t=0.001$ and $t=100$ on the same plot we rescale them in such a way that the characteristic widths of the distributions $W(t)$, defined by $\int_0^{W(t)} f(x,t)dx=1/4$, are the same. One can see an excellent fit to exact result. Note that the value of β_{eff} grows monotonously with time, while the value of D_{eff} exhibits a nonmonotonous behavior, first rising up to the value of 2 and then decaying toward 1.

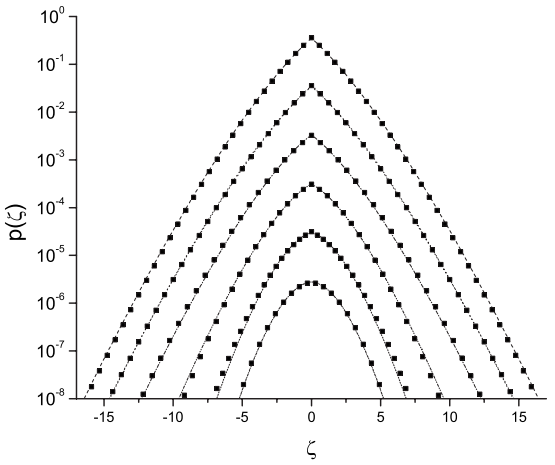

FIG. 6. The rescaled PDF $p(\zeta)=W(t)f(x,t)$, where $f(x,t)$ is obtained by inverse Laplace transform of Eq. (29), is shown for different values of ζ as a function of rescaled displacement $\zeta=x/W(t)$, for different time instants, from top to bottom: $t=0.001$, 0.01, 0.1, 1.0, 10, and 100. The corresponding dashed lines demonstrate the single-order solution given by Eq. (25) with the parameters, from top to bottom, $\beta_{\text{eff}}=0.5$, 0.5, 0.6, 0.73, 0.8, 0.95; $D_{\text{eff}}=1$, 1.05, 1.7, 1.95, 2.0, 1.4.

III. DISCUSSION

There are several observations in which subdiffusion behavior changes into normal one in the course of time. We mention below some of them. In experiments [29] the Lagrangian velocity of tracer particles was measured in a turbulent flow with the use of ultrasonic Doppler tracking. The PDFs of velocity increments were almost Gaussian at integral time scales and progressively developed stretched exponential tails for small time increments. This is a manifestation of intermittency. In order to explain these experiments, in the paper [30] time-fractional single-order diffusion equation in d dimensions was obtained, starting from the Navier-Stokes equation. Its solution was compared with the PDF measured experimentally. It was shown that the experimental PDF can be well reproduced at each time instant by fixing a definite value of the fractional order exponent, which is a free parameter of the theory. The fitting values of the exponent vary between approximately 0.5 for small time and 1.0 for long time; see Fig. 1 in [30]. Our results allow us to suggest that, in principle, another explanation could be possible, with appropriate generalization of a double-order diffusion equation and its solution to a three-dimensional case.

Analysis of the mean squared displacements data from single-particle tracking experiments with membrane-bound proteins revealed transition from subdiffusion to normal diffusion [31,32]. It was shown in [32] that this transition can be understood in terms of subdiffusion mechanism punctuated by occasional Lévy flights. Biological mechanisms of the transition from subdiffusion at small times to normal diffusion at large times are discussed in [33].

Another related example comes from the single-file diffusion which occurs when particles moving in one-dimensional space cannot pass one another. This notion was originally introduced to describe the transport of ions through narrow channels in biological membranes [34]. In particular, such kind of diffusion was also found in zeolites, which are complex, crystalline inorganic materials widely used in petrochemical and industrial processes [35]. Recent molecular dynamics simulations extended to the nanosecond scale revealed subdiffusive behavior obeying non-Gaussian statistics in different crystalline microporous aluminosilicates and demonstrated availability of fractional diffusion interpretation of simulated single-file diffusion in microporous materials [36,37]. For a comparison between the propagator obtained from molecular dynamics simulations and that of a single-order diffusion equation the instantaneous values of fractional order and diffusion coefficients were fitted to the simulated MSD. It was suggested in Ref. [37] that the distributed order equation may be employed for an alternative description of the phenomenon.

At last, we note that the transition from slower subdiffusion to faster subdiffusion can be seen in the measurements of subdiffusion parameters provided in Refs. [38,39]. Indeed, one can clearly observe in Fig. 2 from Ref. [38] that for experiments with glucose at small times the experimentally measured thickness of the near membrane layer as a function of time grows slower than at long times, at which the subdiffusion exponent 0.9 is obtained with good accuracy.

Summarizing Sec. II, the presented analysis and the discussion allows us to conclude that the modified distributed order time-fractional diffusion equation may be a useful tool for the description of the phenomena demonstrating anomalous subdiffusion behavior at small times and normal diffusion at large times. In the next section we demonstrate how the modified distributed-order space-fractional diffusion equation describes transient superdiffusion phenomena.

IV. MODIFIED DISTRIBUTED-ORDER SPACE-FRACTIONAL DIFFUSION EQUATION

A. General equations

Let us consider the diffusionlike equation with an additional distributed-order space fractional operator on the left-hand side [3]:

$$\int_0^2 d\alpha p(\alpha) l^{2-\alpha} \frac{\partial^{2-\alpha}}{\partial |x|^{2-\alpha}} \frac{\partial f}{\partial t} = -D \frac{\partial^2 f}{\partial x^2}, \quad 0 < \alpha \leq 2, \quad (37)$$

where $[l]=\text{cm}$, $[D]=\text{cm}^2/\text{sec}$, and the length l is introduced in such a way that $p(\alpha)$ is a dimensionless non-negative generalized function obeying the normalization condition $\int_0^2 d\alpha p(\alpha)=1$, possibly having delta points in $0<\alpha\leq 2$, but not at $\alpha=0$. Here, $\partial^\mu/\partial|x|^\mu$ denotes a symmetric Riesz derivative (we adopt here the notation introduced in [40]), which, for a "sufficiently well-behaved" function $\phi(x)$ is defined through the Liouville-Weyl derivatives [41,27,42]:

$$\frac{d^\mu}{d|x|^\mu}\phi(x) = \begin{cases} -\dfrac{1}{2\cos(\pi\mu/2)}[D_+^\mu\phi + D_-^\mu\phi], & 0<\mu\le 2, \quad \mu\neq 1 \\ -\dfrac{d}{dx}H\phi, & \mu=1 \\ -\phi, & \mu=0 \end{cases}, \tag{38}$$

where $D_\pm^\alpha$ are the left- and right-side Liouville-Weyl derivatives,

$$D_+^\mu\phi = \frac{1}{\Gamma(m-\alpha)}\frac{d^m}{dx^m}\int_{-\infty}^{x}\frac{\phi(\xi)d\xi}{(\xi-x)^{\alpha-m+1}},$$

$$D_-^\mu\phi = \frac{(-1)^m}{\Gamma(m-\alpha)}\frac{d^m}{dx^m}\int_{x}^{\infty}\frac{\phi(\xi)d\xi}{(x-\xi)^{\alpha-m+1}}, \quad m=[m]+1, \tag{39}$$

where $[\cdots]$ means the integer part of the number (note that $D_\pm^1 = \pm d/dx$ at $\mu=1$). H is the Hilbert transform operator,

$$H\phi = \frac{1}{\pi}\int_{-\infty}^{\infty}\frac{\phi(\xi)d\xi}{x-\xi}. \tag{40}$$

The definitions of $d^\mu/d|x|^\mu$ at $\mu=0$ and $\mu=1$ appear as continuous limits of the general definition [first line of Eq. (38)] for $\mu\to 0$ and $\mu\to 1$, respectively.

In Fourier space the operators of fractional derivatives have a simple form:

$$\mathbf{F}(D_\pm^\alpha\phi) = \int_{-\infty}^{\infty}dx\,\exp(ikx)D_\pm^\alpha\phi = (\mp ik)^\alpha\hat{\phi}(k), \tag{41}$$

where $\mathbf{F}$ denotes the Fourier transform operation, $\hat{\phi}(k)$ is the Fourier transform of $\phi(x)$, and

$$(\mp ik)^\alpha = |k|^\alpha\exp\left(\mp\frac{\alpha\pi i}{2}\operatorname{sgn} k\right).$$

Since

$$\mathbf{F}(H\phi) = i\,\operatorname{sgn} k\,\hat{\phi}, \tag{42}$$

then, with the use of Eqs. (38)–(42) we get an expression, which is valid for the Fourier transform of the Riesz fractional derivative for all α's:

$$\mathbf{F}\left(\frac{d^\alpha\phi}{d|x|^\alpha}\right) = -|k|^\alpha\hat{\phi}. \tag{43}$$

We note here that the Riesz derivative of the order 2 coincides with the second integer derivative. However, the first Riesz derivative does not coincide with the first integer derivative; moreover, the zero order Riesz derivative acting on some function ϕ gives $-\phi$. The latter property will be used in what follows.

Equation (37) is subject to the initial condition $f(x,t=0)=\delta(x)$. Setting $p(\alpha)=\delta(\alpha-2)$ in Eq. (37), we arrive at the usual diffusion equation. Setting $p(\alpha)=\delta(\alpha-\alpha_0)$, $0<\alpha_0\le 2$, we arrive at the space-fractional diffusion equation in a "modified" form [3],

$$\frac{\partial^{2-\alpha_0}}{\partial|x|^{2-\alpha_0}}\frac{\partial f}{\partial t} = -D_{\alpha_0}\frac{\partial^2 f}{\partial x^2}, \tag{44}$$

with $D_{\alpha_0}=D/l^{2-\alpha_0}$. With $\alpha_0=2$ we arrive at the usual diffusion equation due to the property of zeroth order Riesz derivative; see the third line in Eq. (38). Equation (44) is equivalent to the "natural" form of the space-fractional diffusion equation,

$$\frac{\partial f}{\partial t} = D_{\alpha_0}\frac{\partial^{\alpha_0} f}{\partial|x|^{\alpha_0}}. \tag{45}$$

Indeed, applying the Fourier transform to Eqs. (44) and (45), $\hat{f}(k,t)=\int_{-\infty}^{\infty}dx e^{ikx}f(x,t)$, and noting Eq. (43) we get from both equations

$$\hat{f}(k,t) = \exp(-D_{\alpha_0}|k|^{\alpha_0}t), \tag{46}$$

which is the characteristic function of the Lévy stable process [43].

Let us return to the distributed-order Eq. (37). Applying to it the Fourier transform, we get the characteristic function

$$\hat{f}(k,t) = \exp\left[-\frac{Dt}{l^2}R_M(k)\right], \tag{47}$$

where

$$R_M(k) = \int_0^2 d\alpha p(\alpha)(|k|l)^{-\alpha}. \tag{48}$$

It is interesting to note that Eq. (47) is the same as the equation for the Fourier transform of the solution of space-fractional distributed-order diffusion equation in natural form, if we replace $R_M(k)$ by $R(k)=\int_0^2 d\alpha p(\alpha)(|k|l)$; see Eq. (44) in [12]. We already mentioned the similar property of the time fractional solution; see Eqs. (11) and (12) in Sec. II. Note that the solution of Eq. (37) is normalized: $\int_{-\infty}^{\infty}dx f(x,t)=\hat{f}(0,t)=1$.

In what follows, we will be interested in (i) the probability density to stay at the origin, which reads as

$$f(0,t) = \int_{-\infty}^{\infty}dk\hat{f}(k,t), \tag{49}$$

and (ii) fractional-order moments of the PDF, which are given by

$$\langle|x(t)|^q\rangle = \int_{-\infty}^{\infty}dx|x|^q f(x,t). \tag{50}$$

B. Generic case of double-order equation

In what follows we consider the following form of the weight function [compare with Eq. (16)]:

$$p(\alpha) = p_1\delta(\alpha - \alpha_1) + p_2\delta(\alpha - 2), \quad 0 < \alpha_1 < 2. \quad (51)$$

Insert Eq. (51) into Eqs. (37), change the notation α_1 to α, and denote $D/p_2 \equiv D' \to D$, $(p_1/p_2)l^{2-\alpha} \equiv C_\alpha$. Then, Eq. (37) takes the form [3]

$$\left(1 - C_\alpha \frac{\partial^{2-\alpha}}{\partial|x|^{2-\alpha}}\right)\frac{\partial f}{\partial t} = D\frac{\partial^2 f}{\partial x^2}, \quad (52)$$

whose solution with the initial condition $f(x,0)=\delta(x)$ is given by the characteristic function

$$\hat{f}(k,t) = \exp\left(-\frac{D\ k^2 t}{1 + C_\alpha|k|^{2-\alpha}}\right). \quad (53)$$

For the first time Eq. (52) was considered in Ref. [7], where the proof of positivity of the solution was also given. The underlying stochastic process is Markovian, and Eq. (53) shows that its PDF is infinitely divisible [24]. This process can be visualized in discrete time $t=1,2,\ldots,\ n$ as a sum of independent jumps, each with the characteristic function $\hat{f}(k,1)$ given by Eq. (53), for its PDF.

The inverse Fourier transform of Eq. (53) cannot be performed analytically. However, we observe that at k large enough (for small $|x|$), $K_\alpha|k|^{2-\alpha} \gg 1$, the characteristic function has the form

$$\hat{f}(k,t) = \exp\left(-\frac{D}{C_\alpha}|k|^\alpha t\right), \quad (54)$$

i.e., it corresponds to the characteristic function of the Lévy stable distribution, compare Eq. (46). However, the asymptotics of the PDF at large x is determined by the first nonanalytical term in the expansion of Eq. (53) at $k \to 0$, that is by $DC_\alpha t|k|^{4-\alpha}$. By making the inverse Fourier transformation of this term and using the Abel method of summation of an improper integral [44,45], we get

$$f(x,t) \simeq \frac{\Gamma(5-\alpha)\sin(\pi\alpha/2)}{\pi}\frac{DC_\alpha t}{|x|^{(5-\alpha)}}, \quad |x| \to \infty. \quad (55)$$

Since $0<\alpha<2$, the Lévy distribution is truncated by a power law with a power between 3 and 5. Thus the solution of Eq. (52) has a finite second moment and, according to the central limit theorem (slowly!) converges to a Gaussian. The peculiarities of the convergence are considered below.

*Probability density to stay at the origin.*We remind that for the Lévy stable law with index α the probability density to stay at the origin is obtained by inserting Eq. (46) into Eq. (49):

$$f(0,t) = \frac{\Gamma(1/\alpha_0)}{\pi\alpha_0}(D_{\alpha_0}t)^{-1/\alpha_0}. \quad (56)$$

In the case of our double-order Eq. (52) this probability is obtained by inserting Eq. (53) into Eq. (49). The integral is evaluated numerically. It is convenient to observe the convergence to the Gaussian case in the course of time by plotting $f(0,t)$ vs time in a log-log scale. The result of numerical calculation is shown in Fig. 7. Here, the probability density to stay at the origin is shown by the solid line. The dashed-dotted and dashed lines demonstrate the probability density

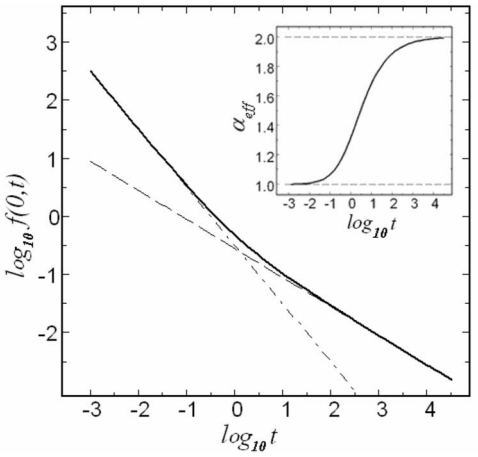

FIG. 7. Solid curve: probability density to stay at the origin obtained by numerical integration of Eq. (53) at $\alpha=1$ (Cauchy distribution), $D=C_1=1$. The dashed-dotted line has the slope corresponding to the Cauchy density, $f(0,t) \sim t^{-1}$. Dashed line has a slope corresponding to the Gaussian distribution, $f(0,t) \sim t^{-1/2}$. The inset demonstrates $\alpha_{\text{eff}}(t)$ obtained from the slope of the solid curve at each time instant.

to stay at the origin for the Cauchy and Gaussian distributions, respectively. One can clearly see the transition from Lévy behavior to a Gaussian behavior. By analogy with Sec. II, we can plot α_{eff} as a function of t, which is obtained from the instant slope of the solid line, that is, $f(0,t) \sim t^{-1/\alpha_{\text{eff}}(t)}$. However, in contrast with Sec. II, it is not possible to approximate the PDF $f(x,t)$ with the Lévy stable PDF with α_{eff} varying in time. The reason lies in the asymptotics, Eq. (55), which is steeper than the asymptotics of the Lévy stable PDF decaying as $|x|^{-1-\alpha}$.

Fractional-order moments. Now, we turn to the moments of the PDF. At first we note that for the power-law truncated Lévy process whose characteristic function is given by Eq. (53) the second moment is finite and displays normal Gaussian diffusion,

$$\langle x^2(t)\rangle = -\left.\frac{\partial^2 \hat{f}(k,t)}{\partial k^2}\right|_{k=0} = 2Dt. \quad (57)$$

However, fractional moments of order $q<2$ demonstrate anomalous non-Gaussian behavior at short times, as we will see below. We remind that for the stable process of the Lévy index α with the characteristic function Eq. (46) the fractional-order moment behaves as [46]

$$\langle|x|^q\rangle = A(q,\alpha)(Dt)^{q/\alpha}, \quad 0 < q < \alpha < 2, \quad (58)$$

where

$$A(q,\alpha) = \frac{2}{\pi q}\sin\left(\frac{\pi q}{2}\right)\Gamma(1+q)\Gamma\left(1-\frac{q}{\alpha}\right).$$

Introducing the root of the order $2/q$ of the qth moment (to have a natural analog for the nonexisting second moment),

$$M_q(t;\alpha) \equiv \langle|x(t)|^q\rangle^{2/q}, \quad (59)$$

we get the for the Lévy stable process from Eq. (58),

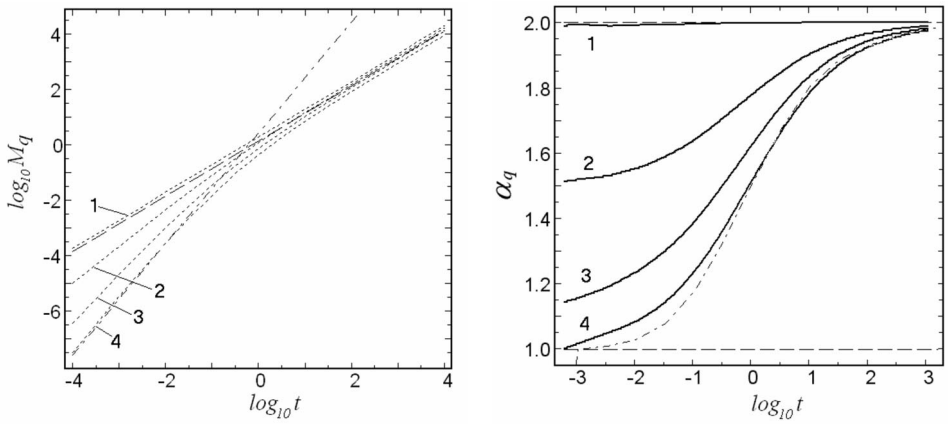

FIG. 8. Left panel: The root of the order $2/q$ of the qth moment, Eq. (59), is shown as a function of t by dotted lines for $q=2.0$, 1.5, 1.0, and 0.5 (lines 1, 2, 3, and 4, respectively). Here, as in Fig. 7, $\alpha=1$, $D=1$, $C_\alpha=1$. The dashed and dashed-dotted lines have tangent of the slope equal to 1 and 2, respectively. Right panel: the quantity $\alpha_q(t)$ defined in Eq. (61) is shown by solid lines 1, 2, 3, and 4 for the same q values as in the left panel. The dashed-dotted line demonstrates α_{eff} from the inset of Fig. 7.

$$M_q(t;\alpha) \propto [A(q,\alpha)]^{2/q} t^{2/\alpha}, \tag{60}$$

that is, this quantity grows faster for $\alpha<2$ than in the Gaussian normal diffusion case, $M_q(t;2)\propto t$, $\alpha=2$. In physics literature this property of fractional-order moments of the Lévy stable process sometimes is attributed to the phenomenon of superdiffusion, that is, the diffusion which is faster than the normal Gaussian diffusion [1]. For Lévy flights the quantity $M_q(t;\alpha)$, Eq. (59), being plotted in a log-log scale, is depicted by a straight line with the tangent of the slope equal to $2/\alpha$, which for $\alpha<2$ is steeper than for the Gaussian case. For our power-law truncated Lévy flights the quantity $M_q(t;a)$ is shown in Fig. 8, left panel, for $q=2.0$, 1.5, 1.0, and 0.5 in a log-log scale. For $q=2$ the tangent of the slope is equal to 1 for all times, which is in agreement with Eq. (57). For order less than 2 the root of the qth moment exhibits steeper slope that is superdiffusive behavior. This property is also demonstrated in a different way in the right panel of Fig. 8. The function $\alpha_q(t)$ shown here is given by

$$\alpha_q(t) = \frac{2}{d[\log_{10} M_q(t;\alpha)]/d(\log_{10} t)}. \tag{61}$$

At short times $\alpha_q(t)<2$. This is the manifestation of a transient superdiffusive behavior, which turns into normal behavior in the course of time. Thus we have a *decelerating superdiffusion*. If we take the value of q less than α ($q<1$ for the process shown in Fig. 8) then we observe that at very short times $\alpha_q(t)\approx\alpha$, see the curve 4 for $q=0.5$. This is a demonstration of a "truly" Lévy behavior at short times of the process considered. Interestingly, the function $\alpha_{0.5}(t)$ is very similar to the function $\alpha_{\text{eff}}(t)$ shown in the inset of Fig. 7 and also depicted in the right panel by the dashed-dotted line.

The property of fractional-order moments to exhibit anomalous non-Gaussian behavior at short times has been recently found for the exponentially truncated Lévy flights [47]. The consequences of this result are the multiscaling properties of the process. Our result confirms this finding and allows us to make the hypothesis that such Lévy-like behavior at small times is inherent for fractional moments of truncated Lévy flights irrespective of the way of truncation.

Time evolution of the PDF. It is interesting to follow the transition from Lévy-like to Gaussian behavior by looking at the evolution of the PDF in time. The PDF obtained numerically by inverse Fourier transform of Eq. (53) is shown in Figs. 9–11. As in previous figures, we take $\alpha=1$, thus we expect to observe the transition of the Cauchy density (or, to be more precise, power-law truncated Cauchy density) into the Gaussian density.

In Fig. 9 the PDF at small time is shown in linear, log-linear, and log-log scale on the left, middle, and right panels, respectively. In the left and right panels the thick solid line showing the shape of the PDF almost completely coincides with the shape of the Cauchy distribution, such that the deviations cannot be visible. The Gaussian distribution is shown here by the dashed line. From the left and middle panels one can see that at the beginning of evolution that is at times small enough the PDF is very close to the Cauchy density. This is true, but for the central part of the PDF, which is only shown in linear and log-linear scales. Looking at the log-log scale (right panel) one can see the deviations from the Cauchy law with x increasing and finally at large x the x^{-4} asymptotics of the truncated Cauchy distribution, Eq. (55).

Figure 10 shows the evolution from Cauchy to Gaussian PDF at intermediate times in linear scale. In the left panel the PDF is still close to the Cauchy PDF, however, one can already see the deviation in the central part. In the middle panel the deviation from the Cauchy density is large, and at the same time the PDF is still far from the Gaussian density. With time increasing (right panel) the PDF becomes closer to Gaussian.

In Fig. 11 the PDF at long time is shown in linear, log-linear, and log-log scales on the left, middle, and right panels, respectively. On the left (linear scale) the PDF (almost) coincides with the Gaussian PDF. Looking at the middle panel (log-linear scale) one can see that such a coincidence takes place in the central part of the PDF only, because at larger x the long tail of the PDF is observed. From the right

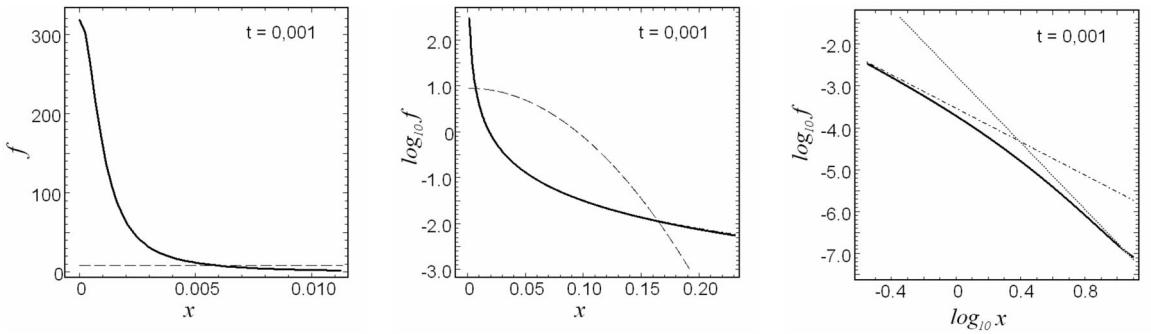

FIG. 9. Thick solid line: PDF $f(x,t)$ obtained by numerical inverse Fourier transform of Eq. (53) at small time $t=0.001$ is shown from left to right in linear, log-linear, and log-log scale. Here $\alpha=1$, $D=1$, $C_\alpha=1$. In the left and middle panels the shape of the Cauchy density almost completely coincides with the PDF depicted by solid line. The Gaussian density at the same time instant is shown here by dashed line. In the right panel the dashed-dotted line indicates the Cauchy density with the tangent of the slope equal −2 and the thin solid line indicates the asymptotics, Eq. (55), with the slope −4.

panel (log-log scale) it is seen that the central Gaussian part is sewn with the power law asymptotics decaying as x^{-4}.

Summarizing the results shown in Figs. 9–11, the evolution of the PDF is as follows. At short times the PDF has a Cauchy shape in the central part and steeper x^{-4} asymptotics. At intermediate times there is a transition from Cauchy shape to the Gaussian shape in the central part. At long times the Gaussian profile is formed in the central part of the PDF whereas the asymptotics is still governed by x^{-4} power law. With further time increasing the central Gaussian part slowly enlarges and, respectively, the beginning of x^{-4} asymptotics is shifted to the larger x values. We note that, different from the subdiffusion case, the PDF at intermediate times is not correctly described by the effective exponent $\alpha_{\text{eff}}(t)$, but shows a more complex behavior, being a combination of the Gaussian (long-time) and Lévy (short-time) ones.

V. DISCUSSION

We point to some possible applications of the power law truncated Lévy flights. In Ref. [48] the fluctuations of floating potential and poloidal electric field have been studied in the boundary plasma of ADITYA tokamak by measuring the probability density to stay at the origin. The transition from the Lévy behavior to Gaussian behavior has been detected. The results were compared with the model of exponentially truncated Lévy flights. However, the very slow convergence to the Gaussian PDF noted in the paper may point to a power law truncation. Actually, Lévy statistics in plasma fluctuations has been also reported for stellarators URAGAN-3M [49] and Heliotron J [50]. The transition from a non-Gaussian statistics with a power-law asymptotics at small time scales to a Gaussian one at large time scales in the central part of the PDF was also reported for plasma density fluctuations in the scrape-off layer plasma of the tokamak HYBTOK-II [51]. We suggest it would be reasonable to revise the analysis of the available plasma data in order to find which truncation procedure seems more adequate.

As another example, a Lévy flight truncated by a faster decaying power law is a much better model for the behavior of commodity prices. Indeed, the discussion in Ref. [52] shows that the cumulative distribution function of cotton prices may correspond to a power-law behavior of $1-F(x)=\int_x^\infty f(x)dx \propto x^{-\alpha}$ with the power $\alpha=1.7$ in its middle part and the far tail decaying as a power law $1-F(x)\propto x^{-\beta}$ with $\beta\approx 3$. Thus our equation (which is definitely the simplest form of the equation for truncated Lévy flights) adequately describes this very interesting case giving $\beta=3.3$. It is highly probable that fractional equations of the type considered here might be a valuable tool in economic research.

One more economical example comes from the analysis of relative changes of stock prices, which over a fixed time interval follow a Lévy stable distribution in the central re-

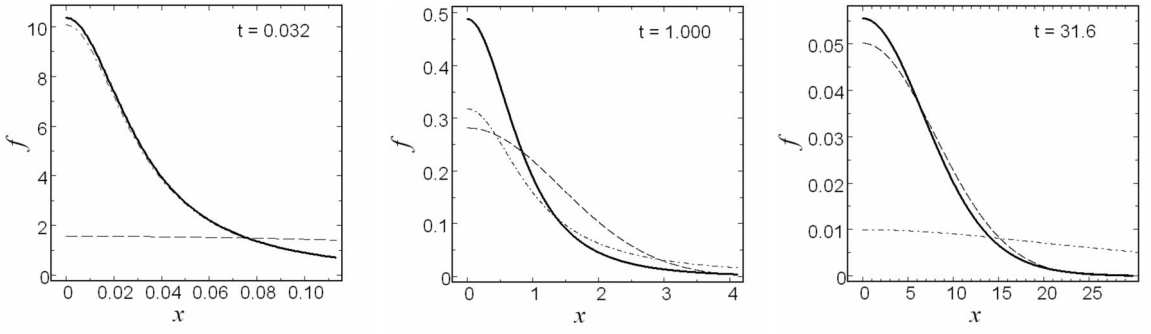

FIG. 10. PDF $f(x,t)$ at intermediate times in linear scale. Here $\alpha=1$, $D=1$, $C_\alpha=1$. Solid line: PDF obtained by inverse Fourier transformation of Eq. (53). Dashed-dotted line: the Cauchy density. Dashed line: the Gaussian density.

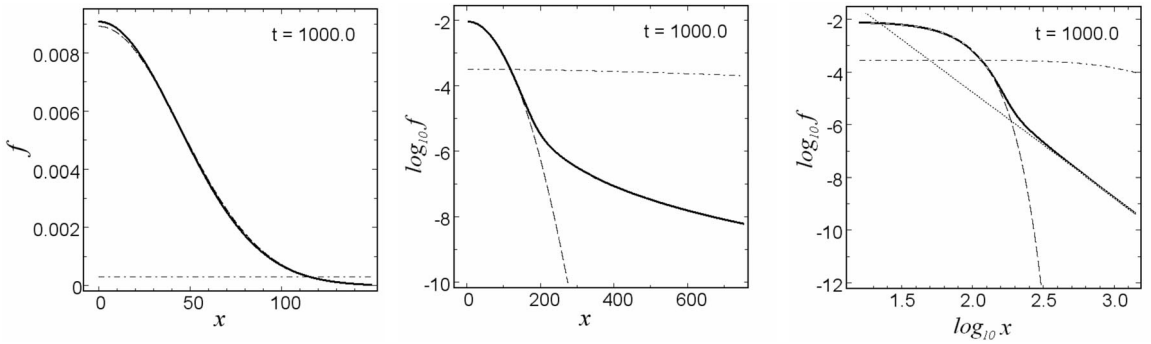

FIG. 11. The PDF $f(x,t)$ at long times, from left to right: linear, log-linear, and log-log scale. Dashed and dashed-dotted line indicate the Gaussian and Cauchy distribution, respectively. The thin solid line in the right panel indicates the asymptotics x^{-4}, Eq. (55).

gion with inverse power law tails [53]. The index α of the Lévy region is approximately 1.4 [54] and the exponent ν of the decay of the tails is typically somewhat less than 4 [55,56]. The high-resolution analysis of a database consisting of 132 000 values of the S&P 500 index taken at 10 min intervals gives $\upsilon = 3.65 \pm 0.21$ [57]. According to our model, $\nu = 5 - \alpha = 3.6$, which nicely agrees with this empirical finding.

VI. SUMMARY

The class of diffusion equations with distributed order derivatives allows us to describe the diffusion processes which are not characterized by a unique exponent related to the order of fractional differentiation or the growth of the mean squared displacement. In the present paper we consider the properties of two diffusion equations, namely, the equation with the distributed order Riemann-Liouville time fractional derivative (accelerating subdiffusion) and the equation with the distributed order Riesz space-fractional derivative (decelerating superdiffusion). We call these two equations modified distributed order diffusion equations in order to distinguish them from those introduced in Ref. [12]. Both equations describe processes which become less anomalous in the course of time. As an important generic example of many distributed orders we consider double-order equations in both cases, containing one integer and one fractional-order term, namely first derivative plus derivative of order less than 1 in a time-fractional equation and second derivative plus fractional of order less than 2 in a space-fractional equation. We study the evolution of the probability density to stay in the origin $f(0,t)$, the MSD $\langle x^2(t) \rangle$, and the PDF $f(x,t)$ itself. Finally, we also provide a discussion about possible applications.

The double-order time fractional diffusion equation describes a subdiffusion process which becomes less subdiffusive (or, in other words, more normal) in the course of time, that is, accelerating subdiffusion. The probability density to stay in the origin exhibits a transition from slow to a faster decay. The MSD demonstrates the transition from the growth characterized by a smaller exponent to the growth with a larger exponent. The PDF evolves from the solution of a single-order diffusion equation with a smaller exponent to the solution of a single-order equation with a larger exponent. We have found that the evolution process can be effectively described by the solution of a single order time-fractional diffusion equation with a fractional exponent varying with time, and we provide a good fit to the solution of a double-order equation by the solution of a single-order equation with time-dependent fractional exponent.

The double-order space fractional diffusion equation describes power-law truncated Lévy flights, that is, a random process showing a slow convergence to a Gaussian, but having Lévy-like behavior at short times. This behavior manifests itself in the non-Gaussian Lévy scaling of the probability density to stay at the origin and in superdiffusive behavior of fractional moments of the order less than 2. At the same time, the MSD exhibits normal growth, i.e., linear in time. The PDF evolves as follows. At short times the central part of the PDF has a Lévy-stable shape, whereas the asymptotics decays with the power law but faster than the decay of the Lévy-stable law. At long times the central part of the PDF approaches more and more to Gaussian shape, however, the asymptotics decay with the same power law. With time increasing the Gaussian central part enlarges.

ACKNOWLEDGMENTS

A.V.C. acknowledges the hospitality of the Department of Mathematics and Informatics at Free University of Berlin and financial support from the Deutsche Forschungsgemeinschaft (DFG). Partial financial support through DFG within the SFB555 joint collaboration program is also gratefully acknowledged.

[1] R. Metzler and J. Klafter, Phys. Rep. **339**, 1 (2000).
[2] I. M. Sokolov, J. Klafter, and A. Blumen, Phys. Today **55**(11), 48 (2002).
[3] I. M. Sokolov, A. V. Chechkin, and J. Klafter, Acta Phys. Pol. B **35**, 1323 (2004).
[4] R. N. Mantegna and H. E. Stanley, Phys. Rev. Lett. **73**, 2946 (1994).
[5] I. Koponen, Phys. Rev. E **52**, 1197 (1995).
[6] Ya. G. Sinai, Theory Probab. Appl. **27**, 256 (1983).
[7] I. M. Sokolov, A. V. Chechkin, and J. Klafter, Physica A **336**, 245 (2004).
[8] A. V. Chechkin, J. Klafter, and I. M. Sokolov, Europhys. Lett. **63**, 326 (2003).
[9] M. Caputo, *Elasticità e Dissipazione* (Zanichelli Printer, Bologna, 1969).
[10] M. Caputo, Ann. Univ. Sez. VII, Sc. Mat. **XLI**, 73 (1995).
[11] M. Caputo, Fractional Calculus Appl. Anal. **4**, 421 (2001).
[12] A. V. Chechkin, R. Gorenflo, and I. M. Sokolov, Phys. Rev. E **66**, 046129 (2002).
[13] I. M. Sokolov and J. Klafter, Chaos **15**, 026103 (2005).
[14] A. V. Chechkin, R. Gorenflo, I. M. Sokolov, and V. Yu. Gonchar, Fractional Calculus Appl. Anal. **6**, 259 (2003).
[15] S. Umarov and R. Gorenflo, Z. Anal. Anw. **24**, 449 (2005).
[16] S. Umarov and S. Steinberg, *IMS Lecture Notes—Monograph Series Vol. 51: High Dimensional Probablility* (Institute of Mathematical Physics, Bethesda, MD, 2006), pp.117–127.
[17] A. N. Kochubei, e-print arXiv:math-ph/0703046v1, J. Math. Anal. Appl. (to be published); e-print arXiv:0710.1710v1, J. Ukr. Mth. J. (to be published).
[18] I. M. Sokolov, Phys. Rev. E **63**, 056111 (2001).
[19] P. Paradisi, R. Cesari, F. Mainardi, and F. Tampieri, Physica A **293**, 130 (2001).
[20] R. Gorenflo and F. Mainardi, in *Fractals and Fractional Calculus in Continuum Mechanics*CISM Courses and Lectures No. 378, edited by A. Carpinteri and F. Mainardi (Springer-Verlag, Wien, New York, 1997), pp. 223–276.
[21] F. Mainardi, A. Mura, G. Pagnini, and R. Gorenflo, e-print arXiv:cond-mat/0701132v1, J. Vib. Control (to be published).
[22] F. Mainardi, A. Mura, G. Pagnini, and R. Gorenflo, in *Mathematical Methods in Engineering*, edited by K. Tas, J. A. Tenreiro-Machado, and D. Baleanu (Springer-Verlag, Dordrecht, 2007), pp. 23–55.
[23] T. A. M. Langlands, Physica A **367**, 136 (2006).
[24] W. Feller, *An Introduction to Probability Theory and its Applications* (Wiley, New York, 1971), Vol. 2.
[25] P. P. Valko and J. Abate, Comput. Math. Appl. **48**, 629 (2004); J. Abate and P. P. Valko Int. J. Numer. Methods Eng. **60**, 979 (2004); P. Valko and J. Abate, Appl. Numer. Math. **53**, 73 (2005).
[26] F. Mainardi and M. Tomirotti, in *Transform Methods and Special Functions*, edited by P. Rusev, I. Dimovski, and V. Kiryakova, Science Culture Technology, Singapore, 1995), pp. 171–183.
[27] I. Podlubny, *Fractional Differential Equations* (Academic Press, San Diego, CA, 1998).
[28] G. Zumofen and J. Klafter, Phys. Rev. E **47**, 851 (1993).
[29] N. Mordant, P. Metz, O. Michel, and J.-F. Pinton, Phys. Rev. Lett. **87**, 214501 (2001); N. Mordant, J. Delour, E. Léveque, A. Arnéodo, and J.-F. Pinton, *ibid.* **89**, 254502 (2002); N. Mordant, J. Delour, E. Léveque, O. Michel, A. Arnéodo, and J.-F. Pinton, J. Stat. Phys. **113**, 701 (2003).
[30] R. Friedrich, Phys. Rev. Lett. **90**, 084501 (2003).
[31] S. Khan, A. M. Reynolds, I. E. G. Morrison, and R. J. Cherry, Phys. Rev. E **71**, 041915 (2005).
[32] A. M. Reynolds, Phys. Lett. A **342**, 439 (2005).
[33] M. J. Saxton, Biophys. J. **92**, 1178 (2007).
[34] A. L. Hodgkin and R. D. Keynes, J. Physiol. **128**, 61 (1955).
[35] J. Kärger and D. M. Ruthven, *Diffusion in Zeolites and Other Microporous Solids* (Wiley, New York, 1992).
[36] P. Demontis, G. Stara, and G. B. Suffritti, J. Chem. Phys. **120**, 9233 (2004).
[37] P. Demontis and G. B. Suffritti, Phys. Rev. E **74**, 051112 (2006).
[38] T. Kosztolowicz, K. Dworecki, and St. Mrowczynski, Phys. Rev. Lett. **94**, 170602 (2005).
[39] T. Kosztolowicz, K. Dworecki, and St. Mrowczynski, Phys. Rev. E **71**, 041105 (2005).
[40] A. I. Saichev and G. M. Zaslavsky, Chaos **7**, 753 (1997).
[41] S. G. Samko, A. A. Kilbas, and O. I. Marichev, *Fractional Integrals and Derivatives, Theory and Applications* (Nauka i Technica, Minsk, 1987), in Russian (English translation: Gordon and Breach, Amsterdam, 1993).
[42] R. Gorenflo and F. Mainardi, in *Problems in Mathematical Physics*, Operator Theory: Advances and Applications No. 121 (Siegfried Prössdorf Memorial Volume), edited by J. Elschner, I. Gohberg, and B. Silbermann (Birkhäuser-Verlag, Basel, Switzerland, 2001), pp. 120–145.
[43] G. Samorodnitsky and M. S. Taqqu, *Stable Non-Gaussian Random Processes* (Chapman & Hall, New York, 1994).
[44] G. H. Hardy, *Divergent Series* (Clarendon, Oxford, 1949).
[45] E. C. Titchmarsh, *Introduction to the Theory of Fourier Integrals* (Chelsea, New York, 1986).
[46] B. J. West and V. Seshadri, Physica A **113**, 203 (1982).
[47] Gy. Terdik, W.A. Woyczynski, and A. Piryatinska, Phys. Lett. A **348**, 94 (2006).
[48] R. Jha, P.K. Kaw, D.R. Kulkarni, J.C. Parikh, and ADITYA Team, Phys. Plasmas **10**, 699 (2003).
[49] V. Yu. Gonchar, A. V. Chechkin, E. D. Sorokovoi, V. V. Chechkin, L. I. Grigor'eva, and E. D. Volkov, Plasma Phys. Rep. **29**, 380 (2003).
[50] T. Mizuuchi *et al.*, J. Nucl. Mater. **337–339**, 332 (2005).
[51] V. Budaev, Y. Kikuchi, Y. Uesugi, and S. Takamura, Nucl. Fusion **44**, S108 (2004).
[52] H. E. Stanley, Physica A **318**, 279 (2003).
[53] R. N. Mantegna and H. E. Stanley, *An Introduction to Econophysics: Correlations and Complexity in Finance* (Cambridge University Press, Cambridge, England, 2000).
[54] R. N. Mantegna and H. E. Stanley, Nature (London) **376**, 46 (1995).
[55] P. Gopikrishnan, M. Meyer, L. A. N. Amaral, and H. E. Stanley, Eur. Phys. J. B **3**, 139 (1998).
[56] X. Gabaix, P. Gopikrishnan, V. Plerou, and H. E. Stanley, Nature (London) **423**, 267 (2003).
[57] M. H. Cohen and P. Venkatesh, in *Practical Fruits of Econophysics. Proceedings of the Third Nikkei Econophysics Symposium*, edited by H. Takayasu (Springer-Verlag, Tokyo, 2006), pp.147–151).